

# Numerical modelling of a repeated fault slip

by S.J. WEBBER\*

## SYNOPSIS

This paper reports on the use of the MINSIM-D stress-analysis program for the modelling of two large seismic events that occurred on the same fault eleven years apart.

It was found that the first event (magnitude 5,2) could not be ascribed to purely mining-induced stresses, indicating that the largest seismic events probably result from the interaction of mining-induced stresses with large-scale tectonic stresses. However, the stress changes induced during eleven years of mining were found to be capable of generating sufficient excess shear stress (ESS) to be responsible for the second event (magnitude 4,3). The upper limit for the magnitude of purely mining-induced events was found to be approximately 4,3.

## SAMEVATTING

Hierdie referaat doen verslag oor die gebruik van die MINSIM-D-spanningsontledingsprogram vir die modellering van twee groot seismiese gebeurtenisse wat elf jaar uitmekaar op dieselfde verskuiwing voorgekom het.

Daar is gevind dat die eerste gebeurtenis (grootte 5,2) nie bloot aan mynbougeïnduseerde spannings toegeskryf kon word nie, wat daarop dui dat die grootste seismiese gebeurtenisse waarskynlik die gevolg is van 'n wisselwerking tussen mynbougeïnduseerde spannings en grootskaalse tektoniese spannings. Daar is egter gevind dat die spanningsveranderings wat deur elf jaar se mynbou geïnduseer is, voldoende oormatige skuifspanning kon ontwikkel het om vir die tweede gebeurtenis (grootte 4,3) verantwoordelik te wees.

Daar is gevind dat die boonste perk vir die grootte van suiwer mynbougeïnduseerde gebeurtenisse ongeveer 4,3 is.

## Background

The largest seismic event in South African mining history occurred on Vaal Reefs Gold Mine on the 7th of April, 1977. The event (A257V) was assigned a magnitude of 5,2 by the South African Geological Survey<sup>1</sup>.

Considerable damage resulted to surface structures in the surrounding towns, but there was comparatively little damage to underground workings. Damage to surface structures included broken windows, cracked walls, and severed water pipes. Underground, all access tunnels close to the hypocentre were inaccessible. Scattered falls of ground were recorded over an area of approximately 7 km<sup>2</sup>. A detailed description of the damage is given by Fernandez and Van der Heever<sup>1</sup>.

Approximately eleven years later, on the 5th of January, 1988, a second event—of magnitude 4,3 (event J834V)—occurred on the same fault approximately 300 m from the first event. There was considerable damage to underground workings, and several miners were killed.

These events are of considerable interest since they occurred on the same fault, the second event occurring after a large amount of mining had taken place during the interim. This provided a unique opportunity to study the regeneration of excess shear stress (ESS) on a fault plane and to ascertain whether large events can be attributed solely to mining-induced stresses.

## Mining and Geology

The region in which the events occurred is dissected by two sets of faults. The first set strikes approximately northeast, and the second approximately northwest. The events studied are located on the dominant northwest-striking fault. This fault has a throw of 250 m and dips

at 73 degrees to the northeast. Because of the faulting, the study area is subdivided into four separate windows.

Only a limited amount of scattered mining had occurred in the area when the first event occurred (Fig. 1). The reef to the southwest had been mined to within 50 m of the fault plane, but there had been no significant mining on the northeast or downthrow side of the fault<sup>2</sup>.

In the intervening eleven years a large amount of mining took place on all four reefs. When the second event occurred, mining was adjacent to the fault plane on both sides for strike lengths of approximately 1 km. In fact, ground adjacent to the fault was being extracted when the event occurred.

The location of the events and the mining layouts at the times of occurrence are shown in Fig. 1.

## Seismic History

Prior to the first event, the area had been effectively quiescent. Only seventeen events occurred in the period 1/1/72 to 7/4/77. Of these, three were of magnitude 3 or greater. Twenty-two hours before the mainshock, a small event occurred several hundred metres in the hangingwall. An event of 3,8 magnitude, also in the hangingwall, occurred minutes before<sup>2</sup>. Eighteen aftershocks were recorded in the following six weeks, most of them being located on a lava horizon deep in the footwall. Fig. 2 is a section through the fault showing the foreshocks, mainshock, and aftershocks. The stratigraphy of the area is also shown.

Subsequent to the first event and prior to the second, the area was seismically active (Fig. 1), 304 events being located in the 3200 m by 3200 m modelling area during this period. Seventeen of these had a magnitude of 3,0 or greater, and six were of magnitude 4,0 or greater. The largest event had a magnitude of 4,5. This occurred 1700 m from A257V and J834V on a different fault.

\* Rock Engineering Laboratory, Chamber of Mines Research Organization, P.O. Box 91230, Auckland Park, 2006 Transvaal.  
© The South African Institute of Mining and Metallurgy, 1990. SA ISSN 0038-223X/3.00 + 0.00. Paper received 12th Feb., 1990.

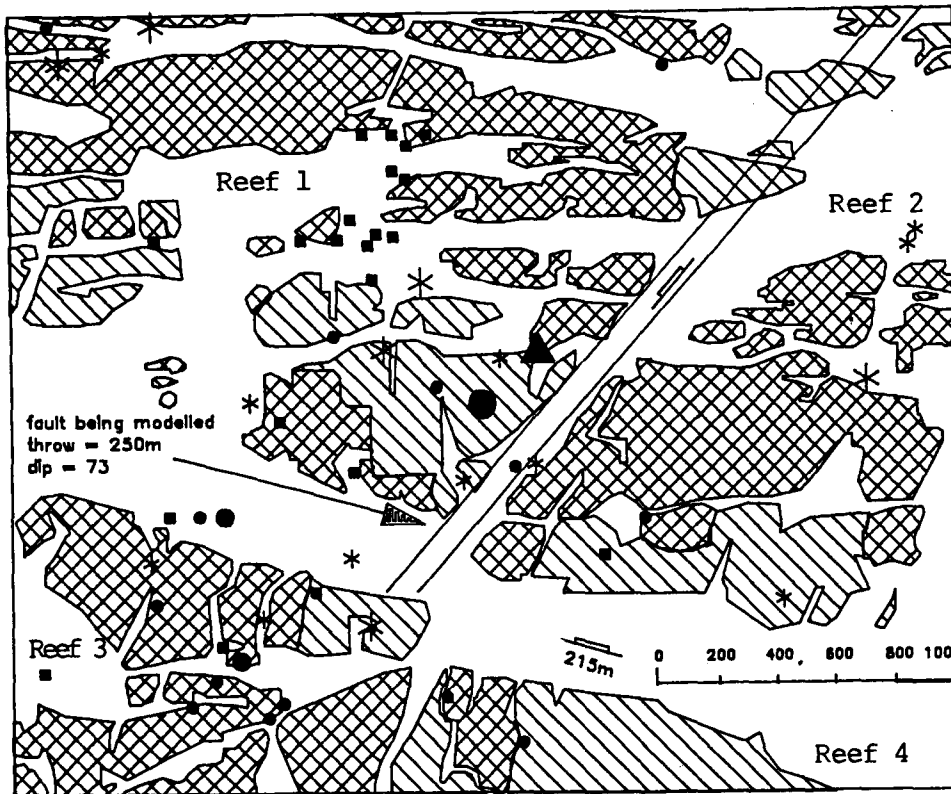
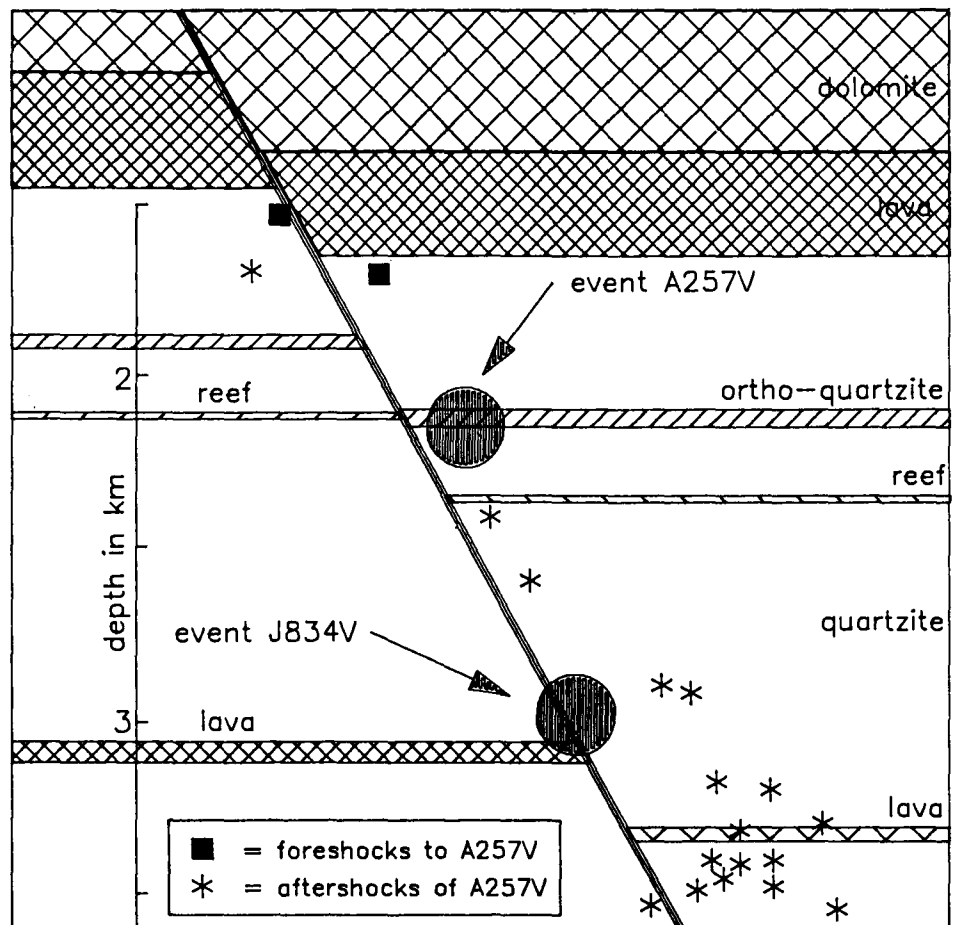


Fig. 1—The mining layout modelled as scenario 1. Also shown are the epicentres of events A257V and J834V, and the seismic activity during the period of study

- Seismicity
- $M < 3,0$
  - $M \geq 3,0$
- } prior to A257V
- A257V
  - Aftershocks
  - \*  $3,0 \leq M < 4,0$
  - \*  $M \geq 4,0$
  - ▲ J834V
- ▨ 1977 faces
  - ▧ 1988 faces

Fig. 2—A section through the fault showing the locations of events A257V and J834V (adapted from Gay *et al.*<sup>2</sup>)



Events of greater magnitude than 3,0 are shown in Fig. 1.

There were no obvious precursors to J834V, and only one event could unambiguously be called an aftershock. The event, with a magnitude of 2,9, occurred 25 hours after the mainshock and 240 m from it. The mainshock was located by the Klerksdorp Regional Seismic Network (K.R.S.N.) approximately 500 m in the footwall. Relocation using raytracing techniques placed the event 70 m in the footwall<sup>3</sup>.

The *b* value derived from the frequency-magnitude distribution was found to be 0,46. This is close to that of the entire mining district, indicating that the seismic activity of the study area is not uncharacteristic of the mining district as a whole<sup>4</sup>.

**Method of Analysis**

Both seismic events were modelled by use of the MINSIM-D suite of programs. (Napier and Stephansen<sup>5</sup> give details of this approach.) Two methods of estimating seismic moment were utilized: calculations based on ESS levels prior to slip, and 'explicit slip' modelling. MINSIM-D allows the computation of ESS at any specified position within the mining window. Explicit slip can be simulated by the modelling of a fault as a completely mined window with an infinitesimally small stoping width and a cohesion of 0 MPa. MINSIM-D requires that the fault being modelled is planar.

Numerical modelling was undertaken for three distinct mining scenarios. The first of these involved digitizing of the mining as it appeared on the mine plan. The second scenario ignored small pillars and remnants. In essence, this assumes that these are crushed and incapable of bearing any load. MINSIM-D assumes that pillars and remnants behave elastically and have infinite strength. However, it is known that this is often not the case

(e.g. Ozbay and Ryder<sup>6</sup>). The third scenario involved 'straightening' of the faces relative to the fault (ignoring small pillars and remnants). Mining takes place right up to the fault trace. The mining layouts modelled in these three scenarios are shown in Figs. 1, 3, and 4.

The magnitude of a potential seismic event that would result from slip over a given area of positive ESS can be calculated by combining a relationship devised by Ryder<sup>7</sup> with the moment-magnitude relationship of Hanks and Kanamori<sup>8</sup>, as follows.

The area of positive ESS is related to the seismic moment of a potential event by

$$M_0 = 2\tau_c a^2 l, \dots\dots\dots (1) \text{ Ryder}^7$$

where  $M_0$  is the seismic moment,  $\tau_c$  is the maximum ESS, and  $a$  and  $l$  are the halfwidth and the strike length of the ESS lobe respectively. It should be noted that, strictly speaking, equation (1) applies only to two-dimensional lobes.

Seismic moment can be written

$$M_0 = \mu AD, \dots\dots\dots (2) \text{ Aki}^9$$

where  $A$  is the area over which the average displacement or slip,  $D$ , occurred, and  $\mu$  is the shear modulus (taken to be  $3,5 \times 10^{10} \text{ Nm}^{-2}$ , Van der Heever<sup>10</sup>).

Hanks and Kanamori<sup>8</sup> devised a moment-magnitude scale for California that has been shown to be appropriate for mining-induced seismic events in South Africa<sup>4</sup>, i.e.

$$\log M_0 = 1,5M + 9,1, \dots\dots (3) \text{ Hanks and Kanamori}^8$$

where  $M$  is the magnitude of the event.

Substitution for  $M_0$  in (3) from (1) and re-arrangement give

$$M = \frac{\log 2\tau_c a^2 l}{1,5} - 6,07. \dots\dots\dots (4)$$

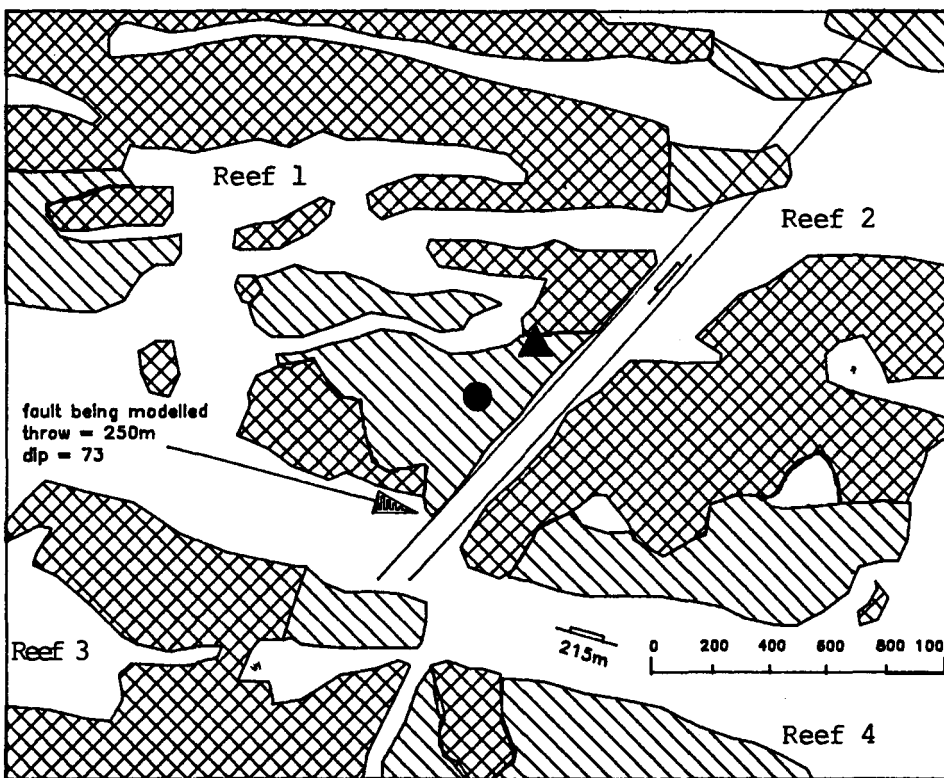


Fig. 3—The mining layout modelled as scenario 2

▨ 1977 faces  
▧ 1988 faces



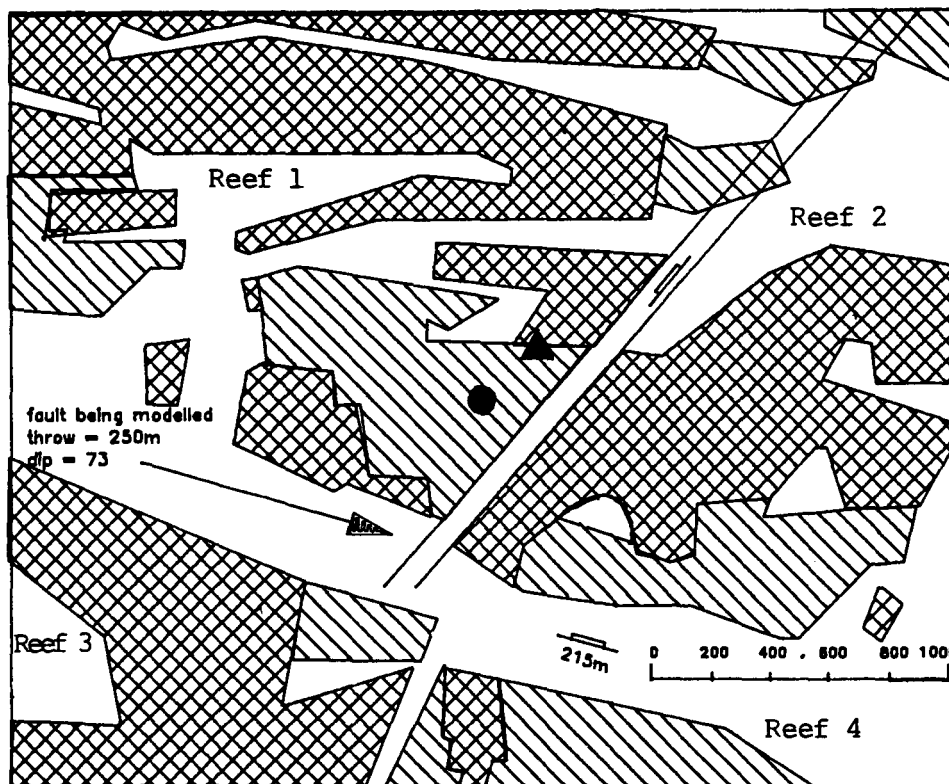


Fig. 4—The mining layout modelled as scenario 3

 1977 faces  
 1988 faces



Thus, for a given area of positive ESS, the magnitude of the seismic event likely to result from the ESS distribution can be calculated from equation (4).

In explicit slip modelling, the magnitude of the event causing the slip can be calculated from equation (2).

#### Input Parameters

As both events occurred on the same fault, the 'step function' facility of MINSIM-D was used. This facility allows incremental mining layouts to be modelled using the solutions of previous layouts. The modelling procedure can be summarized as follows.

- (1) Solve the base run (1977 face positions) and compute ESS on the fault plane.
- (2) Allow the fault to slip and compute the ride distribution.
- (3) Increment the mining (1988 face positions), clamp the fault by using a cohesion of 100 MPa, and solve. Clamping the fault allows the incremental ESS to be calculated.
- (4) Allow the fault to slip again and compute the ride distribution.

These four steps were performed for ratios of the horizontal to vertical stress,  $k$ , of 0,4 and 0,5 and for each of the three scenarios. Clearly, these simulations could be undertaken for a number of such ratios. Van der Heever<sup>10</sup> and Gay and Van der Heever<sup>11</sup> found that, in Klerksdorp,  $k$  varied from 0,68 to 1,0, and that there was a marked horizontal stress anisotropy. Ryder *et al.*<sup>12</sup> found that  $k$  was as high as 1,5 in isolated areas.

In the absence of stress measurements,  $k$  for modelling purposes is usually assumed to be 0,5 in the Klerksdorp mining district. However, it has become clear that the use of this value results in gross differences between

the magnitude determined by modelling and that of the actual event<sup>6,13</sup>. Consequently, although each scenario was modelled both for  $k = 0,4$  and  $k = 0,5$ , only the contour plots of scenarios 1 and 3 for  $k = 0,4$  are presented here. The results for  $k = 0,5$  and scenario 2 are presented in Tables I to IV.

For a friction angle of 30 degrees, the critical  $k$  value is 0,33 (Ryder<sup>7</sup>). If the virgin stress ratio falls below  $k_{critical}$ , then massive normal slip must take place over geological time to relax regional shear stresses and thereby increase  $k$  to a more stable value. The  $k$  value was changed by adjustment of the horizontal stress.

The input parameters were as follows:

Grid size	50 m
Poisson's ratio	0,19
Young's modulus	78 GPa
Friction angle	30°
Cohesion	0
Stoping width	1,2 m
<i>Reef dips:</i>	
Reef 1	10°
Reef 2	9°
Reef 3	15°
Reef 4	18°

When the step function is used the previous slip is embedded on the slip plane, in the benchmark output. Consequently, the incremental seismic moment is derived by subtraction of the original moment from the moment at step 1.

#### Results and Discussion

##### Event A257V ( $M = 5,2$ )

The ESS distributions on the fault plane for scenarios 1 and 3 are shown in Figs. 5 and 6 respectively. These

clearly show the effects of omitting pillars and remnants, and of straightening the faces. The area of positive ESS is increased by a factor of 3,2 for scenario 2 and by a factor of 4,6 for scenario 3 (Table I).

TABLE I  
POSITIVE ESS AREAS AND ESTIMATED MAGNITUDES FOR EVENT A257V

	Positive ESS m <sup>2</sup>	Potential magnitude
Scenario 1: $k = 0,5$	—	Not determined
$k = 0,4$	$1,93 \times 10^5$	3,7
Scenario 2: $k = 0,5$	$3,28 \times 10^5$	4,1
$k = 0,4$	$6,23 \times 10^5$	4,5
Scenario 3: $k = 0,5$	$5,95 \times 10^5$	4,2
$k = 0,4$	$8,80 \times 10^5$	4,5

It should be noted that Figs. 5 and 6 refer to a  $k$  value of 0,4. The effect of  $k$  on the area of positive ESS and the potential magnitude of the event are demonstrated in Table I.

The results of the explicit slip modelling are shown in Table II, and the  $Y$  (dip-slip) component of ride resulting from the ESS distributions in Figs. 5 and 6 are shown in Figs. 7 and 8. From these, it is clear that the slip area is substantially larger in each case than the ESS area generating the slip.

The results displayed in Tables I and II clearly show that it is not possible to adequately model an event of 5,2 magnitude using MINSIM-D without making gross

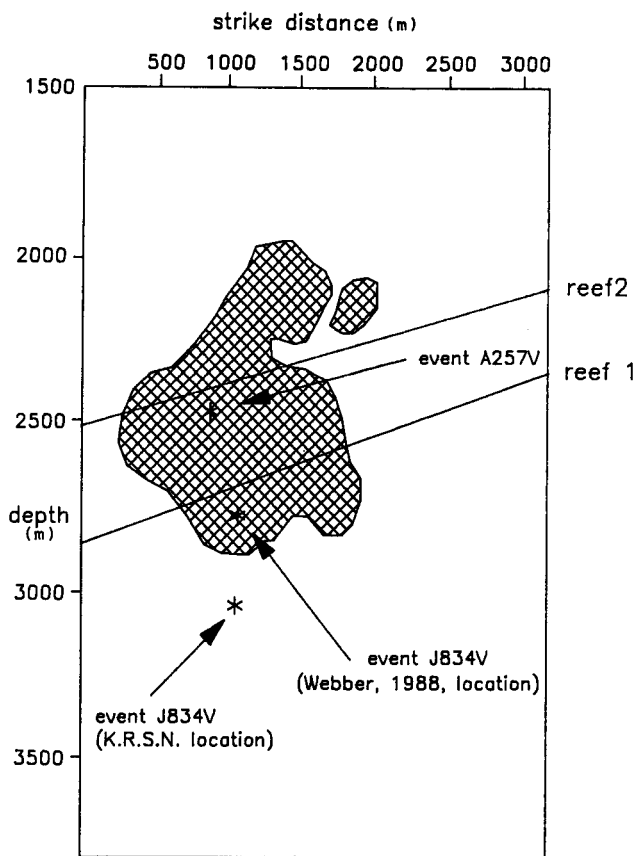


Fig. 6—ESS on the fault plane in scenario 3,  $k = 0,4$ , event A257V (the hatched area is positive)

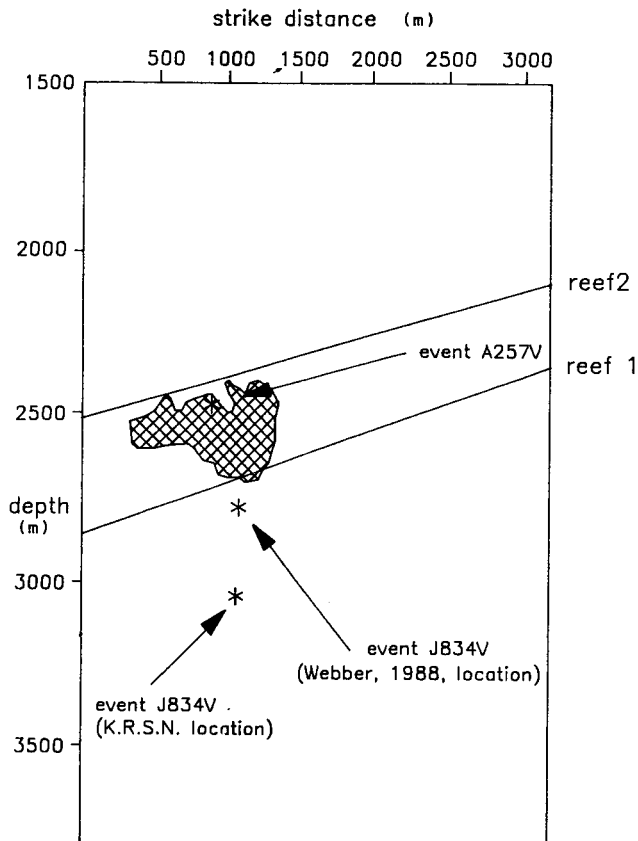


Fig. 5—ESS on the fault plane in scenario 1,  $k = 0,4$ , event A257V (the hatched area is positive)

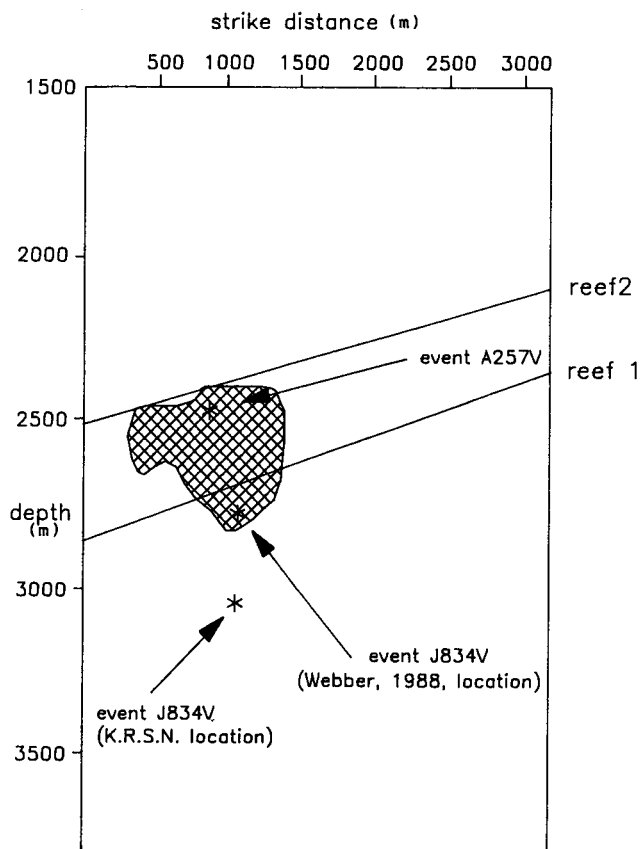


Fig. 7—The  $Y$  component of ride for scenario 1,  $k = 0,4$ , event A257V (the hatched area is slip in the normal sense)

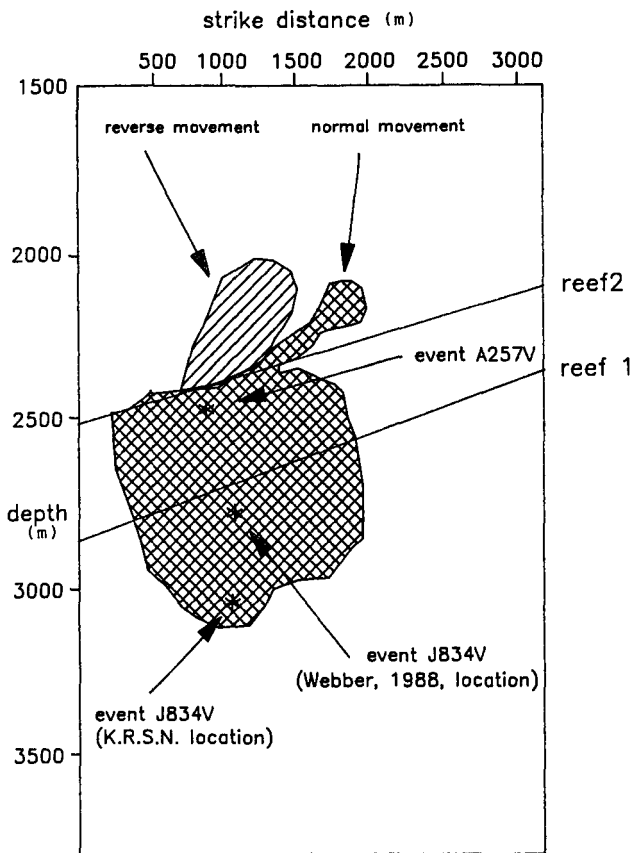


Fig. 8—The Y component of ride for scenario 3,  $k = 0,4$ , event A257V (the hatched area is slip in the normal sense)

TABLE II  
SUMMARY OF EXPLICIT-SLIP MODELLING RESULTS FOR EVENT A257V

	Slip area $m^2$	Maximum slip mm	Magnitude of slip
Scenario 1: $k = 0,5$	$7,0 \times 10^4$	9	2,4
$k = 0,4$	$2,9 \times 10^5$	40	3,4
Scenario 2: $k = 0,5$	$3,1 \times 10^5$	70	3,5
$k = 0,4$	$7,6 \times 10^5$	140	3,9
Scenario 3: $k = 0,5$	$5,1 \times 10^5$	90	3,8
$k = 0,4$	$1,0 \times 10^6$	180	4,1

assumptions. This suggests that very large events cannot be ascribed purely to mining-induced stresses. In essence, there must be an additional energy source.

Gay *et al.*<sup>2</sup> hypothesized that the largest events are due to the interaction of mining-induced stresses and large-scale tectonic stresses, i.e. mining activity disturbs the potentially unstable, pre-mining equilibrium by superimposing small mining-induced stresses on the prevailing stress field. In addition, Ryder *et al.*<sup>12</sup>, contended, from two dimensional modelling, that the magnitude of the largest event that can result from purely mining-induced stresses is approximately 3,5. Although the results of the present study support the assertion of an upper magnitude limit on mining-induced events, the actual limit proposed by Ryder *et al.*<sup>12</sup> is debatable.

#### Event J834V ( $M = 4,3$ )

The ESS regenerated by eleven years of mining, is

shown for scenarios 1 and 3 in Figs. 9 and 10 respectively. From these, it is clear that a considerable area of positive ESS has been re-established in each case. However, for scenario 1, positive ESS has not been regenerated over much of the fault-loss area that slipped previously. (A similar pattern was observed for scenario 2.) Also, in scenario 3 (Fig. 10), there is an area of negative ESS on the fault loss. In each scenario, the maximum amplitude of the ESS was approximately twice that originally present. The results of the ESS modelling are summarized in Table III.

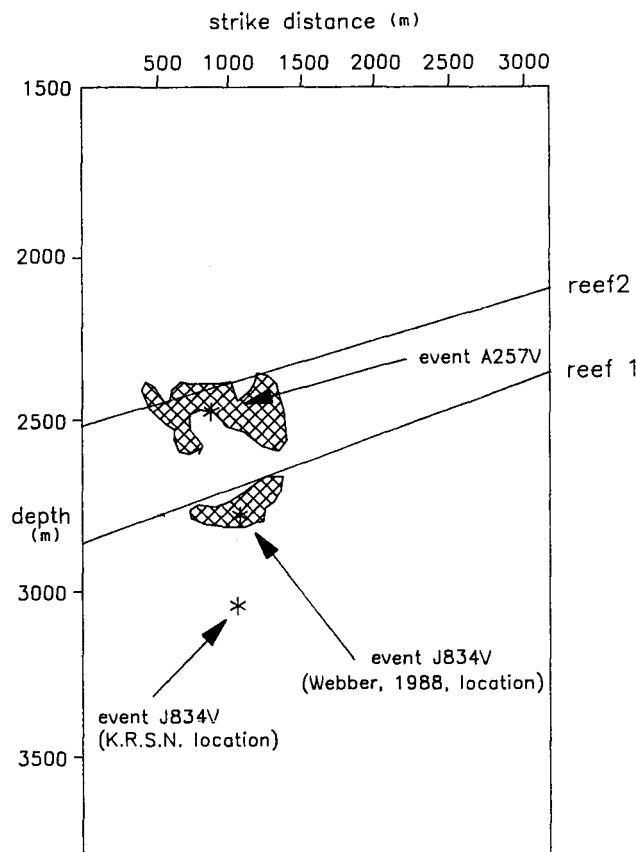


Fig. 9—Regenerated ESS on the fault plane for scenario 1,  $k = 0,4$ , event J834V (the hatched area is positive)

TABLE III  
POSITIVE ESS AREAS AND ESTIMATED MAGNITUDES FOR EVENT J834V

	Positive ESS $m^2$	Potential magnitude
Scenario 1: $k = 0,5$	$4,75 \times 10^5$	Not determined
$k = 0,4$	$1,80 \times 10^5$	Not determined
Scenario 2: $k = 0,5$	$5,58 \times 10^5$	4,6
$k = 0,4$	$9,38 \times 10^5$	4,7
Scenario 3: $k = 0,5$	$8,40 \times 10^5$	4,8
$k = 0,4$	$1,36 \times 10^6$	4,8

From Table III it is evident that the ESS distributions over-estimate the actual magnitude of 4,3. Strictly speaking, equation (4) applies only to two-dimensional rectangular or elliptical lobes<sup>7</sup>. The ESS distributions of Figs. 9 and 10 differ significantly from ellipticity or rec-

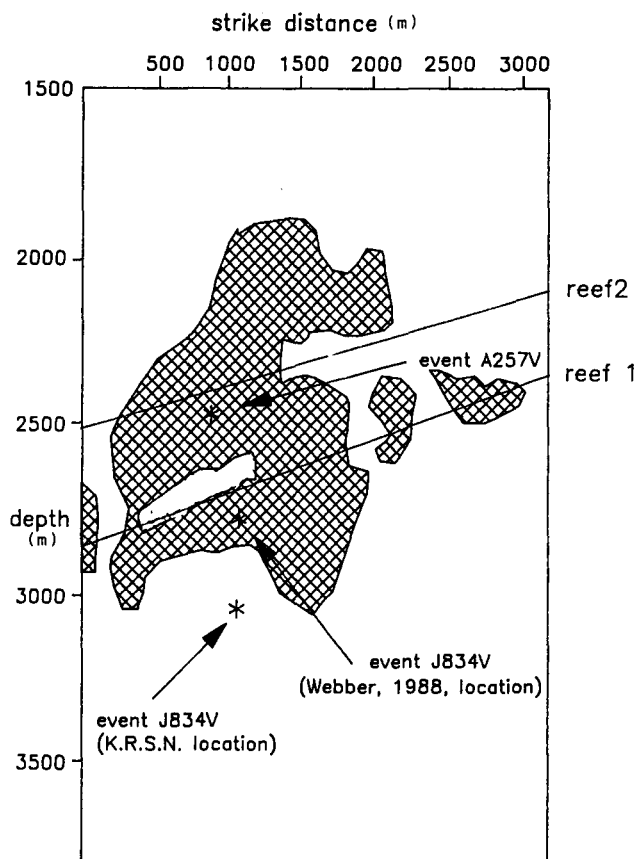


Fig. 10—Regenerated ESS on the fault plane for scenario 3,  $k = 0,4$ , event J834V (the hatched area is positive)

tangularity. Also, the irregular shapes of the lobes make it difficult to estimate the half-widths and lengths required by equation (4). Consequently, the use of equation (4) may not be justified in these cases.

The Y components of ride summed over both events are shown for scenarios 1 and 3 in Figs. 11 and 12 respectively. The step function of MINSIM-D displays the total ride distribution, and not that of the second event only. This makes it difficult to investigate the slip due to regenerated ESS. Nevertheless, from a comparison of Figs. 11 and 12 with Figs. 7 and 8 respectively, it is clear that in each case the slip has occurred higher in the hangingwall, deeper in the footwall, and over a greater strike extent, than previously.

It is significant that the area of reverse slip has decreased (Fig. 12). After the first event the shear stresses in the hangingwall were oriented up the fault plane so as to induce reverse slip. In the fault loss and footwall, the shear stresses were oriented down the fault plane so as to induce normal movement. In a stress environment in which  $k$  is less than 1,0, the natural propensity for fault movement is in the normal sense. This sense of movement would have been inhibited by the shear-stress orientation in the hangingwall after the first event.

The maximum magnitudes of total slip and incremental slip are summarized in Table IV. It should be noted that *total slip area* refers to the total area that slipped over both events. *Maximum total slip* refers to the grid point at which the slip, summed over both events, was the greatest. *Magnitude of incremental slip* refers to the slip generated in the second event, and is calculated by sub-

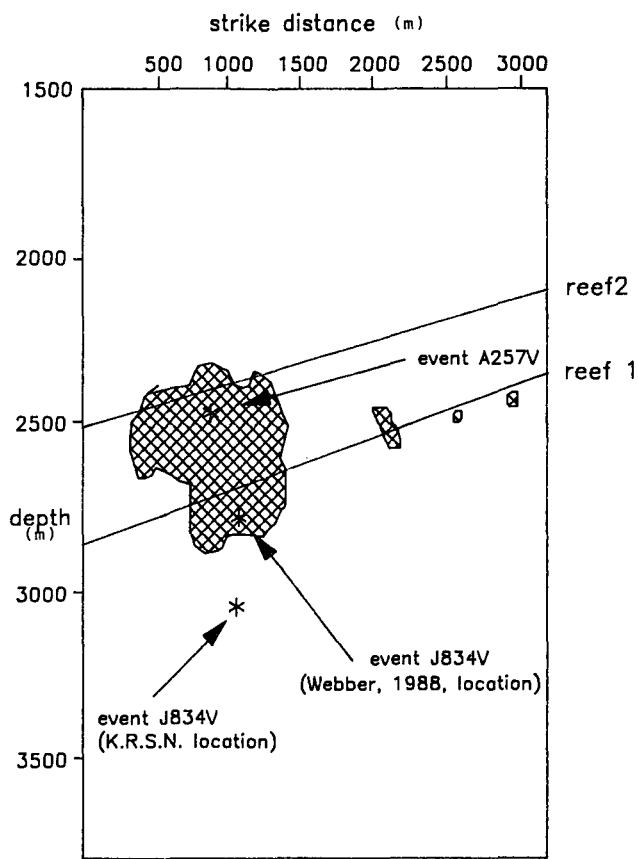


Fig. 11—The total Y component of ride for scenario 1,  $k = 0,4$ , summed over both events

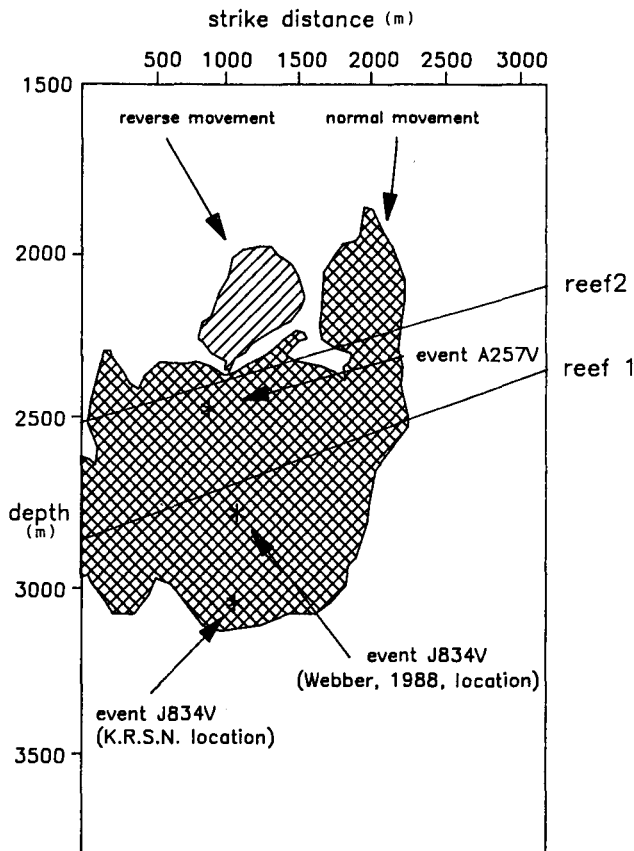


Fig. 12—The total Y component of ride for scenario 3,  $k = 0,4$ , summed over both events

TABLE IV  
SUMMARY OF EXPLICIT-SLIP MODELLING RESULTS FOR EVENT  
J834V

	Total slip area m <sup>2</sup>	Maximum total slip mm	Magnitude of incremental slip
Scenario 1: $k = 0,5$	$1,2 \times 10^5$	22	2,8
$k = 0,4$	$3,7 \times 10^5$	50	3,1
Scenario 2: $k = 0,5$	$7,8 \times 10^5$	80	3,8
$k = 0,4$	$1,7 \times 10^5$	180	4,2
Scenario 3: $k = 0,5$	$7,3 \times 10^5$	260	4,0
$k = 0,4$	$1,5 \times 10^6$	375	4,2

traction of the moment of the first event from the total moment.

As can be seen from Table IV, the magnitudes obtained for scenarios 2 and 3 agree well with the actual magnitude of the event, particularly when it is noted that the uncertainties in the determination of regional or national network magnitudes are generally regarded as  $\pm 0,2$  at best (e.g. Lee and Stewart<sup>14</sup>). This particular event was assigned a magnitude of 4,05, with a standard deviation of 0,79, by the South African Geological Survey<sup>15</sup>.

The results summarized in Table IV clearly demonstrate that it is possible to adequately model repeated fault slip using the MINSIM-D suite of programs without making grossly unrealistic assumptions.

As mentioned previously, it is known that the value of  $k$  in the Klerksdorp mining district varies significantly. Consequently, the choice of the most appropriate value of  $k$  for modelling purposes is problematical.

The present study shows that the value chosen for  $k$  has an enormous effect on the ESS and slip distribution on a fault plane. An alternative to the adjustment of  $k$  is adjustment of the friction angle. Lowering the friction angle will increase the ESS, slip areas, and amplitudes. Little research has been undertaken into the effect of friction angle on the ESS distribution. However, preliminary investigations have shown that a lowering of the friction angle to 22 degrees from the value of 30 degrees assumed here increases the seismic moment by almost two orders of magnitude<sup>16</sup>.

### Conclusion

It was found that the very largest seismic events cannot be considered to result purely from mining-induced stresses. These events probably result from the superimposition of mining-induced stresses on large-scale tectonic stresses. A more complete knowledge of the tectonic-stress tensor would allow large events to be modelled successfully.

The event of largest magnitude that can be modelled without invoking tectonic stresses was found to approximate 4,2 to 4,3.

Repeated fault slip due to the regeneration of mining-induced ESS was successfully modelled using MINSIM-D. However, the effects of mining rate and location on ESS regeneration on the fault are still not clear. An understanding of the mechanisms involved in ESS regeneration is essential if progress is to be made in quantifying the relationships between mining and seismicity.

The lack of fault planarity, and the inelastic behaviour of pillars and remnants, appear to have significant effects

on the ESS distribution on the fault plane. Criteria need to be developed to reduce the arbitrary nature of the procedures of fault 'straightening' and pillar or remnant 'crushing'.

The choice of  $k$  value was shown to significantly influence the ESS and slip distributions. A  $k$  value of 0,4 is probably suitable for the modelling of large events in scattered mining environments.

An alternative to the adjustment of  $k$  value is a change in friction angle. The effects of the friction angle on ESS distribution still require much study before a suitable criterion can be derived for modelling.

### Acknowledgements

This work forms part of the research programme of the Chamber of Mines Research Organization (COMRO). Permission to publish is gratefully acknowledged. Thanks are also due to Vaal Reefs Gold Mine for permission to publish these results, and to Dr J. Coggan of Vaal Reefs Rock Mechanics Department for several helpful discussions.

### References

- FERNANDEZ, L.M., and VAN DER HEEVER, P.K. Ground movement and damage accompanying a large seismic event in the Klerksdorp district. Proceedings of the First International Congress on Rockbursts and Seismicity in Mines, Johannesburg, 1982.
- GAY, N.C., SPENCER, D., VAN WYK, J.J., and VAN DER HEEVER, P.K. The control of geological and mining parameters in the Klerksdorp mining district. *Ibid.*
- WEBBER, S.J. Raytracing in faulted ground. Proceedings of the Second International Symposium on Rockbursts and Seismicity in Mines, Minneapolis (USA), June 1988.
- WEBBER, S.J. Seismic moments and volume changes in the Klerksdorp goldfields. Unpublished Chamber of Mines research report, 1989.
- NAPIER, J.A.L., and STEPHANSEN, S.J. Analysis of deep-level mine design problems using the MINSIM-D boundary element problem. *APCOM 87. Proceedings of the Twentieth International Symposium on the Application of Computers and Mathematics in the Mineral Industries*. Johannesburg, South African Institute of Mining and Metallurgy, 1987. vol. 1, pp. 3-19.
- OZBAY, M.U., and RYDER, J.A. ESS back analysis of a large seismic event (Hartebeestfontein, January 1983, magnitude 4.0). Unpublished Chamber of Mines technical note, 1986.
- RYDER, J.A. Excess shear stress assessment of geologically hazardous situations. *J. S. Afr. Inst. Min. Metall.*, vol. 88. 1988. pp. 27-39.
- HANKS, T., and KANAMORI, H. A moment-magnitude scale. *J. Geophys. Res.*, vol. 84. 1979. pp. 2348-2350.
- AKI, K. Generation and propagation of G-waves from the Nigata earthquake of June 16 1964. Part 2: Estimation of earthquake moment, released energy, and stress drop from the G-wave spectrum. *Bull. Earthq. Res. Inst.*, Tokyo University, 1966.
- VAN DER HEEVER, P.K. The influence of geologic structure on seismicity and rockbursts in the Klerksdorp Goldfield. Unpublished M.Sc. thesis, Rand Afrikaans University, Johannesburg, 1982.
- GAY, N.C., and VAN DER HEEVER, P.K. *In situ* stresses in the Klerksdorp gold mining district, South Africa—a correlation between geological structure and seismicity. Proceedings of 23rd Symposium on Rock Mechanics, University of California (USA), 1982.
- RYDER, J.A., LING, T., and WAGNER, H. Slippage along a fault plane as a rockburst mechanism-static analysis. Unpublished Chamber of Mines Research Report 31/78. 1978.
- WEBBER, S.J. Numerical modelling of a large seismic event. Unpublished Chamber of Mines research report, 1989.
- LEE, W.H.K., and STEWART, S.W. Principles and applications of microearthquake networks. *Advances in Geophysics*, Supplement 2. Academic Press, 1981.
- GEOLOGICAL SURVEY, SOUTH AFRICA. *Seismological Bulletin. Report no. 1988-0047*. Jan. 1988.
- WEBBER, S.J. Unpublished data, 1989.